# ENERGY TRANSPORT MECHANISMS IN PARTICLE-LADEN TURBULENT WATER CHANNEL FLOW

**Yohei Sato**
Mechanical Engineering Systems
National Institute of Advanced Industrial Science and Technology
1-2-1 Namiki, Tsukuba Science City, Ibaraki, 305-8564, JAPAN

**Koichi Hishida**
Department of System Design Engineering
Faculty of Science and Technology
Keio University
3-14-1 Hiyoshi, Kohoku-ku, Yokohama, 223-8522, JAPAN

## ABSTRACT

The mechanisms of energy transport by solid particles in a turbulent water channel flow were investigated by a laser measurement technique and large eddy simulation. Particle image velocimetry was employed to detect particle velocities and fluid information amongst particles. A filtering technique was applied to the fluid flow to extract a characteristic length scale that governs the energy transfer from particles to fluid turbulence. Simulations were performed considering directional scale dependency on force coupling method between particles and turbulence, which can predict both turbulence attenuation and augmentation by particles. An increase in streamwise turbulence intensity in the presence of particles is mainly attributed to increasing values of particle-associated term in fluctuating velocity budget. The energy backscatter due to particles was observed at $\Delta/d_p \approx 10$ ($\Delta$ : filter width, $d_p$ : particle diameter) in both experiments and simulations, which indicates that particles affect the eddy motion whose size is approximately ten times particle diameter.

## INTRODUCTION

Adding solid particles to a turbulent flow dramatically complicates characterization of the flow and renders the traditional empirical methodology for single-phase flow as far from complete. Experimental efforts (e.g., Fleckhaus *et al.* 1987, Rogers and Eaton 1991, Kulick *et al.* 1994, Sato *et al.* 1996) have showed that small particles attenuate fluid turbulence, while large particles augment it. However, the mechanisms responsible for this increase or decrease are still poorly understood. Direct numerical simulation (DNS) (e.g., Squires and Eaton 1990, Elghobashi and Truesdell 1993, Bovin *et al.* 1998) is a powerful tool to advance our understanding, however, these simulations remain restricted to relative low Reynolds number turbulent flows.

The turbulence energy transport due to particles was first examined by Sato and Hishida (1996) who introduced the multiple time-scale concept in their turbulence model. They indicated that large particles have a tendency to become clusters that affect large eddy scale of fluid turbulence, which were supported by their experiments using particle image velocimetry (PIV), and uniformly-dispersed small particles dissipate turbulence kinetic energy, which induces energy cascade from small eddies to dissipative ones (Hishida and Sato 1999). For further insight into the nature of turbulence modification by particles, Sato *et al.* (2000) investigated the distortion process of fluid amongst particles in a vertical downflow water channel by PIV. They found directional scale dependency on turbulence augmentation using the inter-particle spacing. To find out which eddy size particles affect significantly, Sato *et al.* (2001) established the Lagrangian PIV measurement technique. Fluid information amongst particles was filtered in their work to investigate the energy backscatter by particles, which was reflected in modeling directional scale dependency on force coupling in large eddy simulation (LES) (Inoue *et al.* 2001). The most important question, i.e., extracting a characteristic scale that governs energy transport due to particles, has been left unanswered by experimental and numerical studies to this day.

To extend our understanding of the energy transport mechanisms, schematic of turbulence modification by particles in wavenumber space is exhibited in figure 1. For example, a cut-off filter is applied to divide energy power spectrum into grid scale (GS) and subgrid scale (SGS). None of the work, however, has revealed that the relationship between a filter size and the energy forward/backscatter due to particles. It's because that turbulence structure in figure 1(*a*) is completely different from that in figure 1(*b*). When large particles augment turbulence (figure 1(*a*)), turbulence energy is increased in the whole wavenumber region. On the other hand, a decrease in energy is observed except in high wavenumber region for the case of turbulence attenuation by small particles (figure 1(*b*)). A significant outcome of persuasive experiments or simulations will be strongly required.

The objective of the present study is to investigate the mechanisms of energy transport due to particles in a vertical downflow water channel by experiments and simulations. PIV is employed to detect fluid information amongst particles and a box filter is applied to extract a characteristic length scale that governs energy transfer between large and small eddies in the presence of particles. The concept of directional scale dependency on force coupling is implemented in LES to support the

(a)

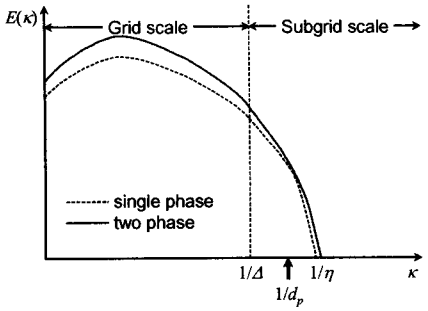


(b)

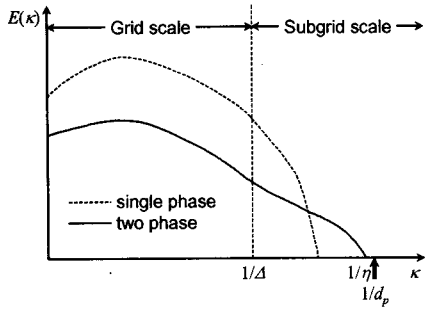


Figure 1. Schematic of turbulence modification by particles in wavenumber space. (*a*) Turbulence augmentation by large particles. (*b*) Turbulence attenuation by small particles.

experimental evidence. From the present work, one can reach a consensus on specifying a characteristic length scale of fluid turbulence which is affected by particles.

## EXPERIMENTAL SETUP

The present experiments were performed in a two-dimensional, vertical channel with downflow of water, identical to that of Sato *et al.* (2000, 2001), as shown in figure 2. The channel was vertically oriented so that the gravitational force on the particles was aligned with the direction of flow. Boundary-layer trips were affixed to both walls at the entrance of a 1.0 m long, 30×250 mm test section. Some of the properties of the flow are presented in table 1. All the experiments were run at a centerline mean velocity of 155 mm/s, corresponding to a Reynolds number of 5,740 based on channel width. The temperature of water was kept constant by using a heater to avoid varying fluid properties. The Kolmogorov micro length scale, $\eta$, at the channel centerline was 252 $\mu$m, which was calculated by direct measurements of dissipation rate of turbulence kinetic energy.

Glass particles were used in the present set of experiments and their characteristics are compiled in table 2. The particle size was chosen with the following strategy: (i) smaller than the energy-containing scale of the flow and (ii) slightly greater than the Kolmogorov micro scale of turbulence. The particle size distributions were determined by using successively smaller sieves, while the particle sphericity was checked by using a microscope.

Velocities of both phases were obtained by using particle image velocimetry (PIV) developed by Sato *et al.* (2000, 2001). Figure 2 shows a schematic illustration of

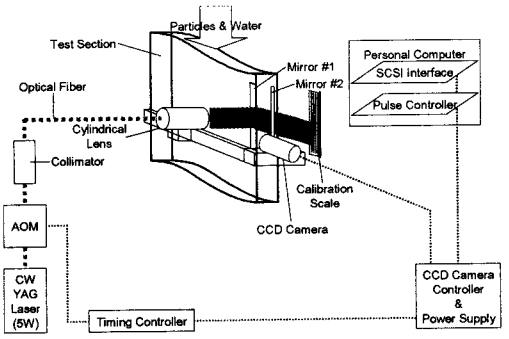


Figure 2. Schematic of particle image velocimetry and vertical water channel.

Table 1. Fluid flow parameters

| | | | |
|---|---|---|---|
| Channel width | $h$ | [mm] | 30 |
| Centerline mean velocity | $\langle U_c \rangle$ | [mm/s] | 155 |
| Channel Reynolds number | $Re_h$ | | 5,740 |
| Kinematic viscosity of water | $\nu$ | [mm$^2$/s] | 0.810 |
| Kolmogorov micro length scale† | $\eta$ | [$\mu$m] | 252 |
| Kolmogorov micro time scale† | $\tau_K$ | [ms] | 78.4 |

†value at channel centerline

Table 2. Properties of particles

| | | | |
|---|---|---|---|
| Material | | | glass |
| Number mean diameter | $d_p$ | [$\mu$m] | 396.4 |
| Stan. dev. of diameter | $\sigma_p$ | [$\mu$m] | 32.3 |
| Density | $\rho_p$ | [kg/m$^3$] | 2,590 |
| Terminal velocity | $V_t$ | [mm/s] | 102 |
| Particle time constant | $\tau_p$ | [ms] | 10.4 |
| Particle Reynolds number‡ | $Re_p$ | | 50.0 |
| Particle mass loading ratio | $\phi_{mass}$ | | $3.3\times10^{-4}$, $8.6\times10^{-4}$ |
| Particle volumetric fraction | $\phi_{vol}$ | | $1.8\times10^{-4}$, $3.3\times10^{-4}$ |

‡mean value calculated by using instantaneous particle Reynolds number

PIV. Velocities were calculated by a cross-correlation technique between two images. Polyethylene particles of 5 $\mu$m (density of 960 kg/m$^3$) were added as tracer particles to the liquid phase. The thickness of the YAG-laser light sheet was 3.0 mm in the test section.

The measurement uncertainty in these experiments was 2.0% for instantaneous velocity measurements. The particles and surrounding fluid were measured by a high-speed CCD camera in a matter of few seconds. Subsequently velocities in time series were calculated within an interval of 1/125 s (= 8 ms).

## OVERVIEW OF THE SIMULATION

The point-force approximation that has been used in DNS and LES can predict turbulence attenuation by small particles reasonably well. In this conventional method, i.e., the momentum is distributed to only eight grid points around a particle, as illustrated in figure 3(*a*), which means that the spatial energy spectrum of fluid around particle(s) is governed by only a grid width in a computational domain. Thus particles always dissipate turbulence energy.

On the other hand, when particles augment turbulence energy, Sato *et al.* (2000, 2001) revealed directional scale dependency on modification to turbulence. This important

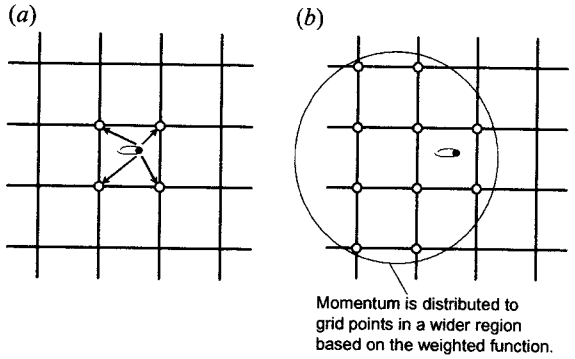


Figure 3. Schematic of force coupling method (*a*) in the conventional point-force approximation and (*b*) considering directional scale dependency concept.

result indicates that the momentum should be distributed to grid points in a wider region, which is exhibited in figure 3(*b*).

From a physical point of view, considering the experimental evidence, the present study introduces the point-force approximation method using a weighted function, that is,

$$w_i(\delta_i) = \frac{1-\alpha\frac{\delta_i^2}{\sigma^2}}{(1-\alpha)\sqrt{2\pi}\sigma} e^{\frac{\delta_i^2}{2\sigma^2}}, \tag{1}$$

where $\delta_i$ is the $i$th-component of nondimensional distance between a grid point and a particle, $\sigma$ is the standard deviation, and $\alpha$ is a factor which defines a function shape over the range of $0 \le \alpha < 1$. If a value of $\alpha$ equals to 0, $w_i(\delta_i)$ becomes the gaussian function, while if $\alpha$ takes a value close to unity, $w_i(\delta_i)$ takes asymptotically the shape of wavelet function. The function $w_i(\delta_i)$ takes on the form,

$$\int_{-\infty}^{\infty} w_i(\delta_i) d\delta_i = 1, \tag{2}$$

which is independent of a value of $\alpha$. During a process of force coupling, the momentum is distributed to grid points in proportional to the integral of weighted function between grid points.

The present simulations solved the following forms of the filtered continuity and Navier-Stokes equations:

$$\frac{\partial \bar{u}_i}{\partial x_i} = 0, \tag{3}$$

$$\frac{\partial \bar{u}_i}{\partial t} + \bar{u}_j \frac{\partial \bar{u}_i}{\partial x_j} = -\frac{1}{\rho_f}\frac{\partial \bar{p}}{\partial x_i} + \frac{\partial}{\partial x_j}\left(\nu \frac{\partial \bar{u}_i}{\partial x_j} - \tau_{ij}\right) - \frac{1}{\rho_f}\bar{f}_{p_i}, \tag{4}$$

where $\bar{u}_i$ and $\bar{p}$ are resolved, i.e., GS, velocity and pressure, and $i$ = 1, 2, 3 denote streamwise ($X$), transverse ($Y$) and spanwise ($Z$) directions respectively, as illustrated in figure 4. The last term in equation (4) is the extra term due to particles calculated by the drag term in the particle motion equation (equation (6)).

The right-hand side of equation (4) contains the SGS stresses that represent the effect of the residual velocity field on the resolved scales and are modeled by using one equation (Yoshizawa and Horiuti 1985):

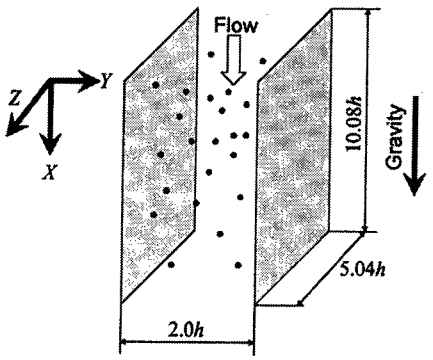


Figure 4. Schematic of calculation domain for LES.

$$\frac{\partial k_{SGS}}{\partial t} + \bar{u}_j \frac{\partial k_{SGS}}{\partial x_j} = 2\nu_e \bar{S}_{ij}\bar{S}_{ij} - c_\varepsilon \frac{k_{SGS}^{3/2}}{\Delta}$$

$$+ \frac{\partial}{\partial x_j}\left(\left(c_{kk}\Delta\sqrt{k_{SGS}} + \nu\right)\frac{\partial k_{SGS}}{\partial x_j}\right). \tag{5}$$

The time-stepping scheme employed the second-order Adams-Bashforth method using the SMAC formulation. Time-stepping errors are small as long as the Courant number is up to 0.15. The spatial-derivative terms were computed by the second-order central finite-difference method. The solution was obtained with 63×48×63 grid points, i.e., uniform grid points in both the streamwise and spanwise directions, while nonuniform in the transverse direction.

The equation of particle motion used in the present study is,

$$\frac{\partial u_{p_i}}{\partial t} = -\frac{u_{r_i}}{\tau_p} - \frac{1}{2}\frac{\rho_f}{\rho_p}\frac{\partial u_{r_i}}{\partial t} + g_i$$

$$+1.615\frac{6}{\pi}\frac{\rho_f}{\rho_p}\frac{1}{d_p}\sqrt{\nu\left|\frac{\partial u_{f_i}}{\partial x_j}\right|}u_{r_i}, \tag{6}$$

where $d_p$ is particle diameter, $C_D$ is the coefficient of drag, $g_i$ is the gravity force and $u_{r_i} = u_{p_i} - u_{f_i}$ is the relative velocity between particle and fluid along the particle path. Interpolation is required to obtain fluid information at a particle point. In the present study the fourth-order accurate Lagrange polynominals were used to interpolate velocities. The Saffman lift force was considered in only the streamwise direction.

Equation (6) was time advanced using the second-order Adams-Bashforth method. Particles were uniformly injected within the computational domain and the inter-particle collisions were neglected. The periodic boundary condition was applied to both the streamwise and spanwise directions, and the elastic collisions were considered at the wall.

Figure 4 shows a schematic illustration of computational domain, in which the periodic boundary condition was applied to both the streamwise and spanwise directions, and the no-slip boundary condition was used at the wall. The grid sizes in the present simulation are $\Delta x$ = 0.16, $\Delta y$ = 0.008–0.08 and $\Delta z$ = 0.08 and the particle diameter conrresponds to $d_p$ = 0.025. Particle volumetric fraction takes a value of $\phi_{vol} = 3.3\times10^{-4}$.

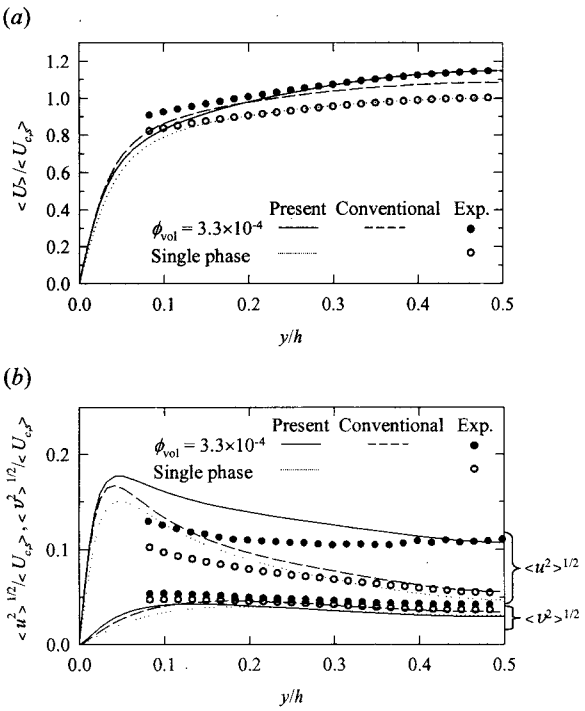


Figure 5. Profiles of (*a*) mean and (*b*) fluctuating streamwise velocities of water. The present method was compared to the conventional point-force approximation method.

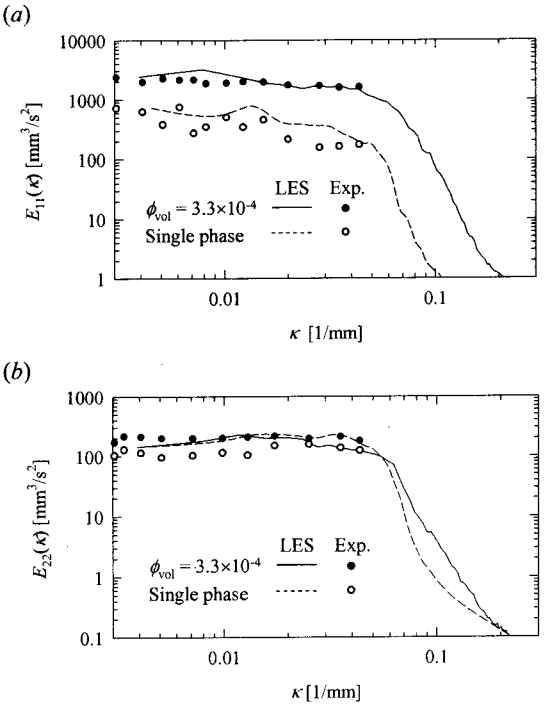


Figure 6. Profiles of velocity power spectra of water at the channel centerline in the presence of particles in the (*a*) streamwise and (*b*) transverse directions.

## RESULTS AND DISCUSSION

### Properties of the flow field

Figure 5 shows profiles of the mean and fluctuating streamwise velocities in the presence of particles obtained from experiments and LES. The coordinate of the figure has nondimensionalized values based on the centerline mean velocity in single phase, $<U_c>$, of 155 m/s and a channel width, $h$, of 30 mm. It is observed at $\phi_{vol} = 3.3\times10^{-4}$ that the mean fluid velocity was accelerated and the fluctuating velocity was significantly augmented especially at the channel centerline. The present force-coupling method shows a significant increase in fluctuating velocity at the channel centerline, which was compared to the conventional method that predicts slight turbulence augmentation.

Further insight into the nature of turbulence modification by particles is provided by the flow power spectra. Figure 6 shows profiles of streamwise and transverse velocity power spectra of water at the centerline of the channel obtained from experiments and LES. The ordinate is normalized by kinematic viscosity of water, $\nu$, and dissipation rate of turbulence kinetic energy of water, $\varepsilon$, in single phase, while the abscissa is normalized by the Kolmogorov micro length scale of water, $\eta$, in single phase. An increase in turbulence energy in the low-wave-number region was observed with an increasing value of particle volumetric fraction, which is identical to the conclusions obtained by Hishida and Sato (1999). LES results show a good agreement with experimental ones, which indicates that directional interactions between particles and turbulence are dominant structure when particles augment turbulence (Sato *et al.* 2000).

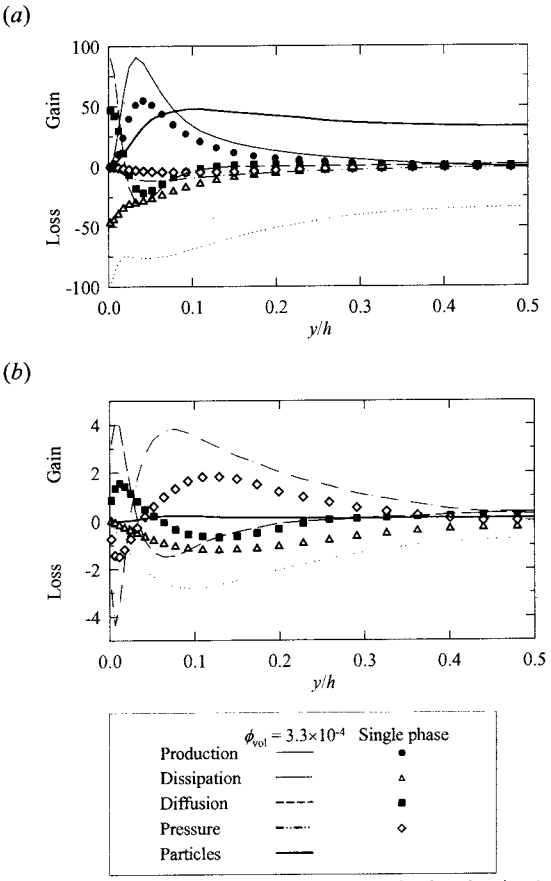


Figure 7. Profiles of fluctuating velocity budget of water in the presence of particles in the (*a*) streamwise, $<uu>$, and (*b*) transverse, $<vv>$, directions obtained from LES. The ordinate is normalized by $u^3_\tau/h$.

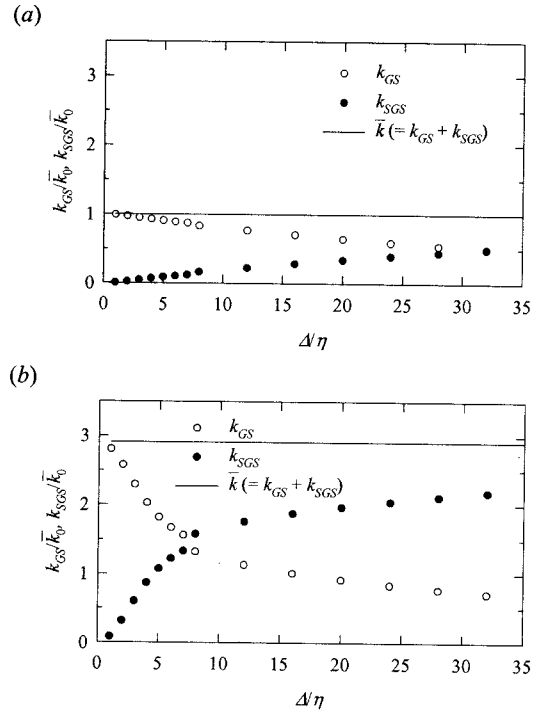


Figure 8. Profiles of the GS and SGS turbulence energy (*a*) in single phase and (*b*) in the presence of particles obtained from experiments. The ordinate is normalized by the summation of $k_{GS}$ and $k_{SGS}$ in single phase, while the abscissa shows the filter width normalized by the Kolmogorov micro length scale.

This important conclusion is supported by figure 7 that exhibits profiles of fluctuating velocity budget of water in the streamwise and transverse directions obtained from LES. The extra term due to particles is balanced with the dissipation rate in the streamwise direction, indicating that particle clusters produce turbulence especially at large-scale eddy motion, which is confirmed by the full DNS (Kajishima and Takiguchi 2001).

## Energy transport by particles

The mechanisms of energy transport by particles in turbulence is analyzed by using a filtering technique in this subsection. A box filter is applied to fluid information amongst particles obtained from PIV measurements (Sato *et al.* 2001).

Figure 8 shows profiles of the GS, $k_{GS}$, and SGS turbulence energy, $k_{SGS}$, as a function of filter width, $\Delta$. The ordinate is normalized by the summation of $k_{GS}$ and $k_{SGS}$ in single phase, $\bar{k}_0$, while the abscissa is normalized by the Kolmogorov micro length scale, $\eta$. In single phase the SGS turbulence energy takes a zero value at $\Delta/\eta = 1$ and is increased with increasing values of the filter width. On the other hand, in the presence of particles the SGS turbulence energy is rapidly increased until $\Delta/\eta \approx 10$ and becomes larger than that in GS at $\Delta/\eta \approx 8$. This means that particles generate eddies whose size, $l$, is over the range of $\eta < l \leq 10\eta$. The summation of turbulence energy, $\bar{k}$, is approximately three times as large as that in single phase, which supports the results in figure 6(*a*).

For further insight into the energy transport mechanisms,

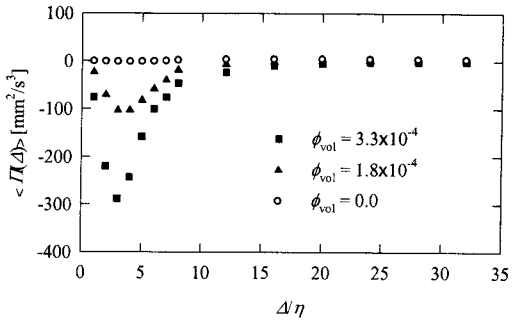


Figure 9. Profiles of energy flux in the presence of particles obtained from experiments. The abscissa shows the filter width normalized by the Kolmogorov micro length scale.

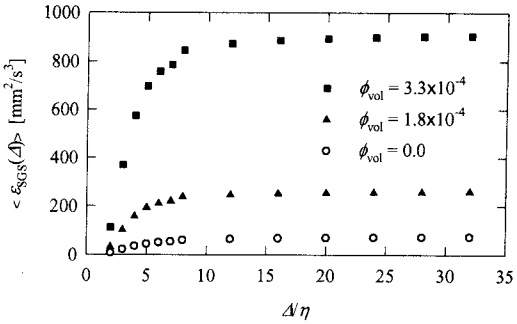


Figure 10. Profiles of SGS energy dissipation rate in the presence of particles obtained from experiments. The abscissa shows the filter width normalized by the Kolmogorov micro length scale.

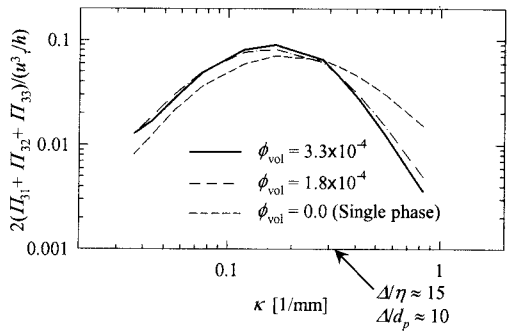


Figure 11. Profiles of energy flux in the presence of particles obtained from LES.

the energy flux, $<\Pi>$, and the SGS energy dissipation rate, $<\varepsilon_{SGS}>$, were calculated by using the filtered velocities. Figure 9 shows profiles of energy flux in the presence of particles as a function of filter width. At $\Delta/\eta \leq 15$ the energy flux takes negative values and this magnitude depends on particle volumetric fraction. This result indicates that the energy backscatter is occurred by particles. When particles augment fluid turbulence, eddies whose size is over the range of $\eta < l \leq 10\eta$ are generated by particles, which induces energy transfer from small scales to large scales. This mechanism is confirmed by results in figure 10 that shows profiles of SGS energy dissipation rate in the presence of particles. The SGS energy dissipation rate is rapidly increased with increasing values of particle volumetric fraction. At $\Delta/\eta \leq 12$ the

dissipation rate takes asymptotic values, because the turbulence energy dissipates significantly at $\Delta/\eta \leq 12$. It is obvious from experiments that particles affect eddies whose size is less than $15\eta$, i.e., $10d_p$.

This important conclusion is also supported by LES. Figure 11 shows profiles of energy flux in the presence of particles obtained from LES considering directional scale dependency on force coupling. The energy flux in the spanwise direction, $2(\Pi_{31} + \Pi_{32} + \Pi_{33})$, is normalized by the friction velocity and the channel width, and is plotted against the wavenumber. The energy backscatter is represented at $\Delta/d_p \approx 10$ ($\Delta/\eta \approx 15$) and is more significant at high volumetric fraction.

The present study focuses on the energy transport mechanisms by solid particles in turbulence using PIV measurements and LES. Both of the works reach a consensus on specifying a characteristic length scale of fluid turbulence which is affected by particles significantly, i.e., particles influence the eddy motion whose size is approximately ten times particle diameter, when particles augment turbulence.

## CONCLUSIONS

PIV measurements and large eddy simulations have been used to investigate the energy transport by solid particles in a turbulent water channel flow. A filtering technique was applied to fluid information amongst particles obtained from experiments to extract a characteristic length scale that governs the energy transfer in the presence of particles. The new force-coupling method considering directional scale dependency was implemented in LES to predict both turbulence attenuation and augmentation. The important conclusions obtained from this work are summarized below.

(1) The turbulence intensity in the streamwise direction, which is identical to the gravity direction, is strongly augmented by particles whose size is slightly greater than the Kolmogorov micro length scale. The extra term due to particles in $<uu>$-transport equation is balanced with the dissipation rate, which means that particle clusters produce turbulence at large-scale eddy motion.

(2) The SGS turbulence energy is rapidly increased until $\Delta/\eta \approx 10$ in the presence of particles, indicating that particles generate eddies whose size is less than $10\eta$.

(3) The energy backscatter due to particles is significant at $\Delta/d_p < 10$, which is confirmed by results of the energy flux and the SGS dissipation rate obtained from PIV measurements.

(4) The present experiments and simulations concluded that interactions between particles and eddy motion whose size is approximately ten times particle diameter induce turbulence augmentation.

## ACKNOWLEDGEMENTS

The authors would like to thank Messrs. H. Inoue and T. Tanaka at Keio University for their performing experiments and simulations.

## REFERENCES

Boivin, M., Simonin, O., and Squires, K.D., 1998, "Direct Numerical Simulation of Turbulence Modification by Particles in Isotropic Turbulence," *Journal of Fluid Mechanics*, Vol. 375, pp. 235–263.

Elghobashi, S.E., and Truesdell, G.C., 1993, "On the Two-Way Interaction between Homogeneous Turbulence and Dispersed Solid Particles. I: Turbulence Modification," *Physics of Fluids A*, Vol. 5, pp. 1790–1801.

Fleckhaus, D., Hishida, K., and Maeda, M., 1987, "Effect of Laden Solid Particles on Turbulent Flow Structure of a Round Free Jet," *Experiments in Fluids*, Vol. 5, pp. 323–333.

Hishida, K., and Sato, Y., 1999, "Turbulence Structure of Dispersed Two-Phase Flows (Measurements by Laser Techniques and Modeling)," *Multiphase Science and Technology*, Vol. 10, pp. 323–346.

Inoue, H., Sato, Y., and Hishida, K., 2001, "Directional Scale Dependency on Force Coupling for Dispersed Two-Phase Turbulent Flows," *Second International Symposium on Turbulence and Shear Flow Phenomena*, Vol. 2, pp. 99–104.

Kajishima, T., and Takiguchi, S., 2001, "Interaction between Particle Clusters and Fluid Turbulence," *Second International Symposium on Turbulence and Shear Flow Phenomena*, Vol. 2, pp. 105–110.

Kulick, J.D., Fessler, J.R., and Eaton, J.K., 1994, "Particle Response and Turbulence Modification in Fully Developed Channel Flow," *Journal of Fluid Mechanics*, Vol. 277, pp. 109–134.

Rogers, C.B., and Eaton, J.K., 1991, "The Effect of Small Particles on Fluid Turbulence in a Flat-Plate Turbulent Boundary Layer in Air," *Physics of Fluids A*, Vol. 3, pp. 928–937.

Sato, Y., Fukuichi, U., and Hishida, K., 2000, "Effect of Inter-Particle Spacing on Turbulence Modification by Lagrangian PIV," *International Journal of Heat and Fluid Flow*, Vol. 21, pp. 554–561.

Sato, Y., and Hishida, K., 1996, "Transport Process of Turbulence Energy in Particle-Laden Turbulent Flow," *International Journal of Heat and Fluid Flow*, Vol. 17, pp. 202–210.

Sato, Y., Hishida, K., and Maeda, M., 1996, "Effect of Dispersed Phase on Modification of Turbulent Flow in a Wall Jet," *ASME Journal of Fluids Engineering*, Vol. 118, pp. 307–315.

Sato, Y., Paris, A.D., Tanaka, T., and Hishida, K., 2001, "Evolution of Subgrid Scale by Particles in a Turbulent Channel Flow Obtained from Lagrangian Measurements," *Second International Symposium on Turbulence and Shear Flow Phenomena*, Vol. 1, pp. 295–300.

Squires, K.D., and Eaton, J.K., 1990, "Particle Response and Turbulence Modification in Isotropic Turbulence," *Physics of Fluids A*, Vol. 2, pp. 1191–1203.

Yoshizawa, A., and Horiuti, K., 1985, "A Statistically-Derived Subgrid-Scale Kinetic Energy Model for Large Eddy Simulation of Turbulent Flows," *Journal Physical Society of Japan*, Vol. 58, No. 8, pp. 2834–2839.